Design and Construction of Electric Wheelchair with Mecanum Wheel

Nuntachai Thongpance [1], Phichitphon Chotikunnan [2*]
[1, 2] College of Biomedical Engineering, Rangsit University, Pathum Thani, Thailand
Email: [1] nuntachai.t@rsu.ac.th, [2] phichitphon.c@rsu.ac.th
*Corresponding Author

Abstract— **This research aimed to design and construct an electric wheelchair with mecanum wheels that can move in any desired direction and speed based on the joystick controller. This represents a significant improvement over traditional electric wheelchairs, which are limited to linear movement in a single direction. The research contribution of this study is the development of an electric wheelchair with mecanum wheels that allows for improved mobility and independence for wheelchair users. The design includes a joystick controller and the use of an average filter to improve the processing of the joystick. This represents a significant improvement over traditional electric wheelchairs, which are limited to linear movement in a single direction. The design and construction of the electric wheelchair followed the ISO 2570-2555 guidelines and utilized Arduino DUE as the main processor for controlling the rotation of the wheels. The gain of speed and angle of the analog joystick were determined using the technique of finding the resultant vector to control the direction and speed of the wheels. The resulting electric wheelchair had a standard structure and was able to move in the desired direction and speed based on the movement of the joystick controller, demonstrating the success of the design and construction in achieving its objective. In conclusion, the development of joystick control for electric wheelchairs is important and allows for the creation of significantly novel and improved designs such as the electric wheelchair with mecanum wheels presented in this research.**

Keywords—Electric Wheelchair; Mecanum Wheel; Joystick Controller; Resultant Vector; Average Filter.

I. INTRODUCTION

Currently, the number of patients with paraplegia or myasthenia gravis and the number of the elderly continues to increase every year. Wheelchairs are popular assistive devices that are commonly found in many places including hospitals. For example, a hand-powered wheelchair is one of the more popular because of its low price but is limited in some areas. Some things for patients or certain types of people because they have to use force from the user or sometimes have to disturb relatives or carers to help. Another type of wheelchair is an electric wheelchair that is very popular both domestically and internationally by using an electric motor to drive. Electric wheelchairs allow users to move more comfortably to their desired destination, but there are some limitations such as difficulty in maneuvering in narrow spaces or with obstacles.

A study has investigated the behavior of wheelchair users to study the body proportions and discomfort levels of physically handicapped workers for the ergonomic requirements of workspace design [1], training in wheelchair use skills, safety, fatigue and wheelchair repair frequency [2], [3], [4], [5], including the emphasis on coaching services, use in public transport areas or problems improving the use of wheelchairs in different areas [6], [7], [8], [9], [10]. It can be seen that most people pay more attention to people who use wheelchairs to move more.

The development of a prototype electric wheelchair device is still a cost problem in the development of prototype devices in terms of mechanics system design, electrical control device design. The Arduino training kit is an alternative way to create a prototype electric wheelchair. In the initial study of prototype development, it can be seen from research on the development of related systems such as motor control systems [11], [12], [13], the development of Autonomous Electric Vehicle using ultrasonic sensors for detecting objects, using the GPS system for navigation and using solar panels to help recharge [14], In addition, the car parking distance controller using ultrasonic sensors [15], includes applications to create small-scale robots that use three degrees of freedom (3-DoF) joints for controlling with a servo motor system [16], Balance robot [17], [18], [19], [20], [21], [22], a line-following robot using a camera sensor pixy II [23], and other related applications such as construction of temperature monitoring system for baby incubator based on visual basic [24], etc.

The design and construction of wheelchairs for people with disabilities has undergone a variety of research and development. For example, the mechanics have been designed autonomous. Stair-climbing wheelchair [25], or a study of the design and construction of an electric wheelchair capable of lifting to maintain the balance system[26], or the development of a wheelchair mechanism, detecting the sitting posture of electric wheelchair users using in-seat pressure measurements [27], the design of a wheelchair motion simulation system to be used as a simulated aid for practicing electric wheelchair driving before actual use [28], [29], [30], [31], creating an electric wheelchair simulation system to simulate the use of a mechanical arm robot in the event that it is installed with the wheelchair to assist in picking things [32].

In the development of the control system for assisting the electric wheelchair, there are various concepts in the design such as the development of an image processing aid system to help drive a wheelchair[33], using LIDAR to autonomous wheelchair [34], building a wheelchair navigation control system for indoor travel [35], map application for wheelchair

users[36], decision-making program for selecting a best compromise direction for a wheelchair [37], a study of speed profiles in wheelchair [38] of wheelchair mobility abilities.

Furthermore, the movement of the electric wheelchair in different directions can be controlled using camera capture techniques and processed using facial expression control techniques [39], hand gesture images [40], or using eye detection images [41], [42], can also be used to control movement. It can also use physical signals such as using the EOG signal in vehicle travel control [43], [44] or the use of soft conformal bioelectronics for a wireless human wheelchair as an interface for visual control [45] or using EEG signals [46], [47] to control the movement of a wheelchair. A wheelchair design for visually impaired persons (for visually impaired persons) has also been designed using the techniques of haptic feedback control of a smart wheelchair [48], [49], [50], [51], [52], [53], for tactile force perception.

The mecanum wheel is an alternative solution to such mobility problems. It has also been applied to create a walking wheelchair. The design of the electric wheelchair can be made by using a computer-aided design model or testing driven electric wheelchair to verify suitability before using it in actual use. In the research conducted on the use of mekanum wheels, the design of mekanum wheels for wheelchairs [54], was studied. Wheelchair with mechanum wheels with adjustable reclining position [55], A mathematical design model of the dynamics of a four-wheeled mobile robot with mecanum wheels [56], which may be found in either the kinematics equations [57] or the Lagrange equation [58]. These equations have been applied to study the design of mecanum wheel layout [59] and kinematic modeling design for use in multiple mecanum-wheeled robots [60]. For the initial control of mechanum wheels, a motion control design may be performed to test the system by means of trajectory tracking control designed [61], [62], [63], [64].

In addition to mechanum wheels, there is also another type of wheel that has the same usage characteristics, this type of wheel is called omnidirectional. wheel, which is a rubber roller wheel that is parallel to the wheel, to research using these wheels for use in wheelchairs, A robot with a technique of placing one wheel in front of the car [65] and using two normal wheels at the back to design a small robot for preliminary locomotion testing. Omnidirectional wheel test [66] to study the pressure data in various forms, which this information can design wheels, wheel holders, and wheel placement to work with full efficiency, design omnidirectional by focusing on the minimization of the gap between the free rollers of the wheel, the efficiency of maneuvering can be improved [67]. There are usually two types of omnidirectional wheel layouts: the use of three omnidirectional wheels in a triangle [68], [69], [70] and the use of omnidirectional. wheel4 pieces are laid out in the shape of a cross [71], [72]. But sometimes it may be placed in the form of a caricature scene [73]. One example of the use of omnidirectional wheels is in the wheeled mobile robots implemented by the Amazon company. These holonomic wheeled robots which are often used to transport goods, which are equipped with omnidirectional wheels that enable

them to move in all directions. [74], [75], [76]. The robot is equipped with omnidirectional wheels that enable it to move in all directions. [77], [78], [79], [80], [81].

The research contribution of this study is the development of an electric wheelchair using mechanum wheels that is able to move in any desired direction and speed based on the joystick controller. This represents a significant improvement over traditional electric wheelchairs, which are limited to linear movement in a single direction. In addition, this study has also contributed to the field by utilizing algorithms, specifically the resultant vector technique and the average filter, to enhance the accuracy and stability of the joystick control system. Another contribution is the proposed use of materials that can be easily obtained in the market and the design of the wheelchair to be easily disassembled, potentially making it more accessible and cost-effective for people with disabilities.

II. METHOD

A. Designing System

The design process for an electric wheelchair with mecanum wheels begins by creating a block diagram to outline the various stages of the design process, as shown in Fig. 1. This process includes designing the system, selecting and designing the hardware, and implementing the entire system.
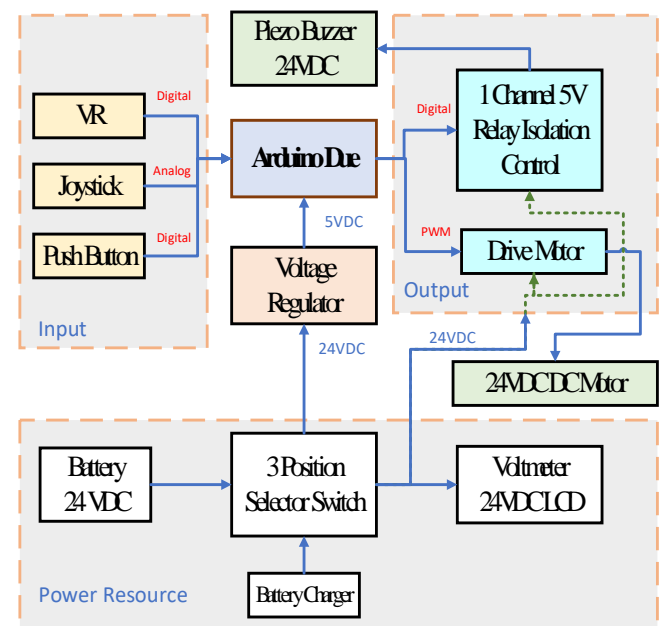
Fig. 1. A block diagram of the structure of the electric wheelchair.

The electric wheelchair system, depicted in Fig. 1, consists of three main components: power resources, input, and output. The power supply for the wheelchair is provided by a 24 VDC battery, which is connected to a 3-way switch that enables or disables the electric wheelchair and allows the user to select a charging mode. The input signals, which are used to control the movement and functionality of the electric wheelchair, are obtained through a joystick with a 10K ohm potentiometer (VR) and a 2-axis controller, all of which are connected to an Arduino Due microcontroller. The DC motor's speed is controlled by these input signals, as well as

a set of 4 H-bridge DC motor driver boards and 4 control boxes, which drive 4 mecanum wheels with 4 motors, also connected to the Arduino Due. An emergency button, connected to the Arduino DUE, is included to activate a horn sound (piezo buzzer) in case of an emergency. The details of these components are described below.

1. Controller box

The main control box of the electric wheelchair processes data from the master joystick to control the left and right motors of the wheelchair. This control box can be programmed with additional information using a USB cable and includes the following components: an Arduino DUE board, a piezo buzzer, four BTS7960 H-Bridge DC Motor Drives, and a 3A Adjustable DC-DC Step-Down power module (LM2596s). The control box is shown in Fig. 2.

Fig. 2. Controller box of the electric wheelchair

2. Joystick Design

To control electric wheelchairs, it is PLA made from a 3D printer in design for controlling an electric wheelchair consisting of display parts, emergency button, system on-off-charger button, potentiometer adjusted speed, the controlling handle for the direction of movement, and movement control buttons as shown in Fig. 3.
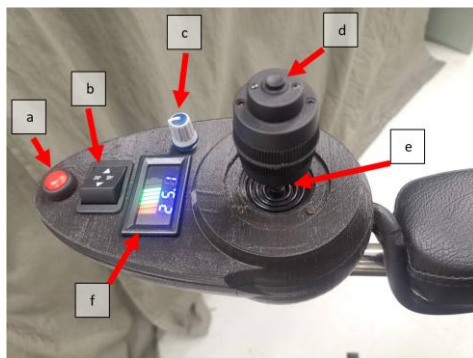
Fig. 3. The details of the joystick for the electric wheelchair.

Electric wheelchair was used to design a joystick for controlling the movement of the motors using mecanum wheels. As shown in Fig. 10, a) point to "emergency button"; b) 3 position selector switch; c) potentiometer; d) shift button of the analog joystick; e) analog joystick; f) voltmeter. The battery compartment is located on the bottom of the joystick base.

3. Potentiometer Joystick 4D direction control Joystick

The potentiometer joystick 4D direction control joystick (RA400A-M2) was used in this research and can be seen in Fig. 4. This joystick allows for more dimensional control of

the direction of the electric wheelchair. Typically, analog 2-axis joystick modules are used to control the movement of electric wheelchairs in four directions. These modules read the values of the X and Y axes through an analog-to-digital converter (ADC) and a microcontroller. The Y axis is usually used to control the movement of the wheelchair forwards and backward, while the X axis is responsible for steering the wheelchair left or right.

Fig. 4. Analog joystick 2 axis.

4. Mecanum Wheel

Mecanum wheels have three degrees of freedom (DOF), enabling them to move in two translational directions along the X and Y axes, as well as one rotational direction around the Z axis. These wheels also have one redundant degree of freedom, which is demonstrated in Fig. 5 [11].

Fig. 5. Mecanum wheels

5. DC Motor

The electric wheelchair uses a DC motor (LX44WG2490) to drive its wheels, as shown in Fig. 6. This motor has a rated torque of 60 Kg. cm at a speed of 71 RPM, and a stall torque of 173 Kg. cm with a load. It operates at a voltage of 24V and has a weight of 0.95 kg. This motor has been selected specifically for use in the electric wheelchair due to its torque and weight capabilities.

Fig. 6. Motor No. LX44WG2490.

B. Mechanical Design

To design an electric wheelchair that is able to move in all directions, SOLIDWORKS 3D CAD simulation modeling software was used to design and analyze the movement of the wheelchair. The design was made in accordance with the ISO 2570-2555 standard and took into consideration the size requirements specified in Table 1, using stainless steel

(SUS304L) as the material. The completed design, shown in Fig. 7, meets all relevant requirements for electric wheelchairs with mecanum wheels, including dimensions of 1100 mm in overall length, 560 mm in overall width, and 890 mm in overall height.

TABLE I. COMPARISON OF DESIGN DIMENSIONS OF ELECTRIC WHEELCHAIRS WITH ISO 2570-2555 REQUIREMENTS

Dimensions	ISO 2570-2555 requirements(mm)	Designed cart size (mm)
Overall length	1, 200	1, 100
Overall width	700	560
Overall height	1, 090	890

Fig. 7. The electric wheelchair with mecanum wheel.

The wheelbase of the electric wheelchair was designed using a computer program to create a structure that allows the wheels to move over various surfaces and can be easily disassembled from the mattress and wheelchair base, as shown in Fig. 8. The system control box and battery are located within the wheelbase, as shown in Fig. 9. Bicycle shock absorbers are installed at four points, and the mecanum wheels and motors are securely fastened together, as shown in Fig. 10.

C. System Flow Chart

The flowchart of the tool's working procedure is shown in Fig. 11. A flowchart is a diagram that visually represents the steps of an algorithm or process, in this case, the proposed system. The set point for this tool is the reading the potentiometer of the joystick in the analog x and analog y values, after which the Arduino reads the initial position. The analog value is then modified and enters a normalization process to process the signal and determine the direction and movement of the system, magnitude or gain (α) and angle

(θ) values. These values are then input into the average filter's processing.
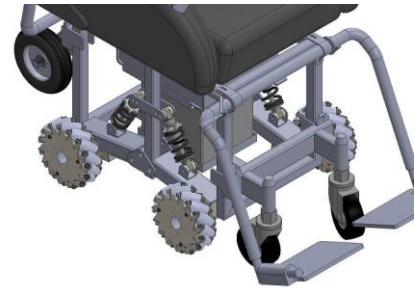
Fig. 8. The wheelbase of the electric wheelchair.
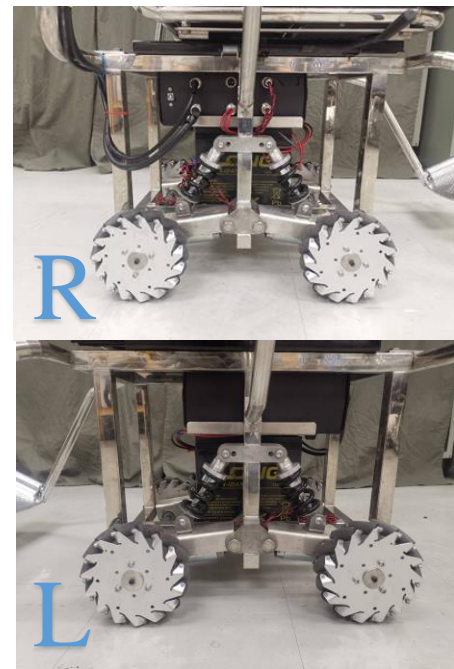
Fig. 9. An example of assembling the wheelbase of an electric wheelchair.

Fig. 10. Assembling the motor part of the electric wheelchair.

Next, the system checks for the pressing of the shift button on the analog joystick. If the angle or direction indicates a slide to the right, the system will slide to the right. If the angle or direction indicates a slide to the left, the system will slide to the left. If the shift button is not pressed and the angle falls within the range of forward, backward, turning right, or turning left, the system will move in the specified direction. Finally, the system checks the value to determine the motor speed and drives the motor at the specified speed, ending the program process.
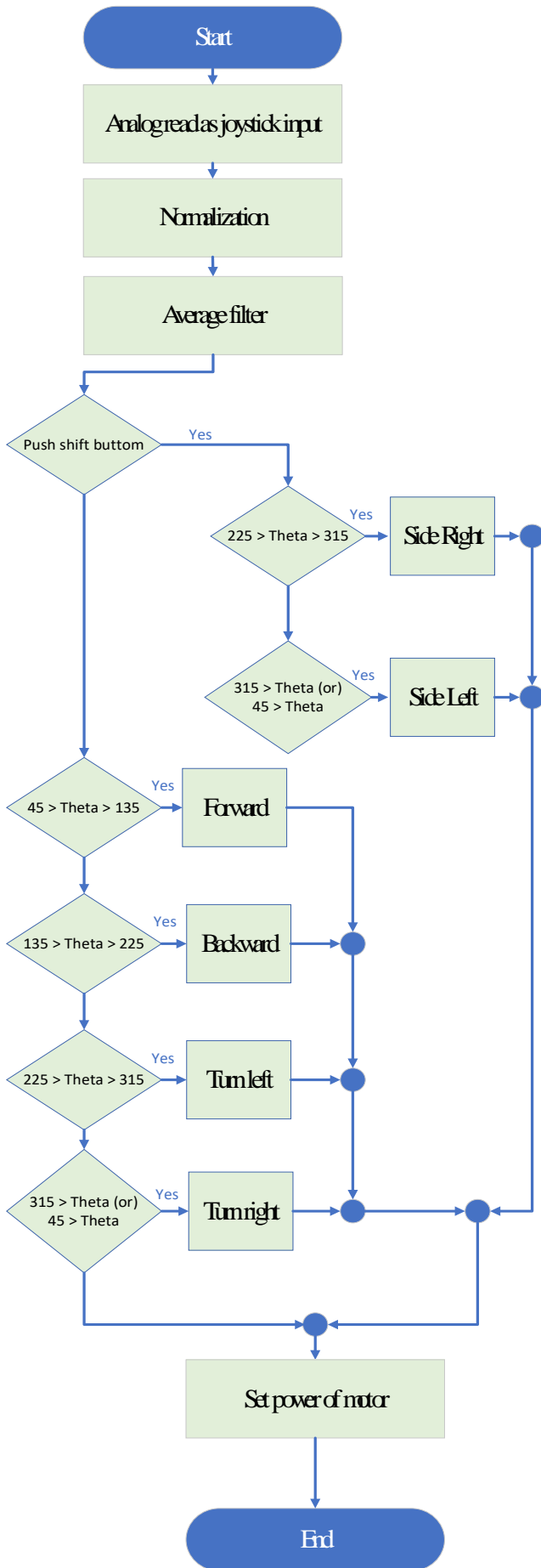
Fig. 11. System Flowchart.

D. Joystick and Mecanum Wheel Control

This section will cover the writing of equations for a program that reads joystick values and uses them to control mecanum wheels. The program will be described in detail as follows.

1. Joystick Control

Fig. 11 illustrates the control sequence of the joystick program. The movement of the wheelchair is shown in Fig. 12 and Fig. 13, with Fig. 12 representing a normal operation, which allows for movement in the forward (F), backward (B), turn right (R), and turn left (L) directions. This operation is only possible when the shift button on the analog joystick is not pressed. If the shift button is pressed, the wheelchair will operate in a special category that allows for only two-way movement, sliding left (SL) and sliding right (SR), as shown in Fig. 13.
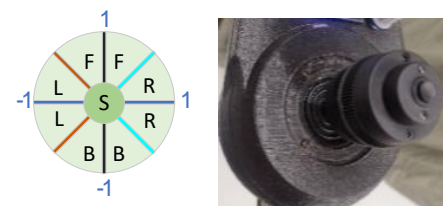
Fig. 12. Programming an analog joystick to allow control of a wheelchair without pressing the shift button.
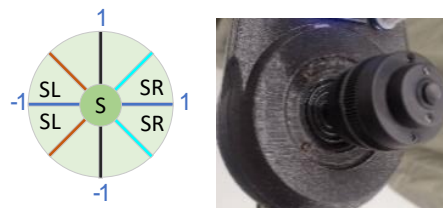
Fig. 13. Programming an analog joystick to allow control of a wheelchair by pressing the shift button.

An analog joystick is often preferred for its ability to directly determine the direction of motion through X-axis and Y-axis readouts. However, this method may not be precise when used to control mechanum wheels. This paper presents the equations and process for converting the analog joystick's signal into a magnitude or gain (α) and angle (θ), which can be used to improve directional control. The input signal from the analog joystick and shift button is processed to normalize the analog signal, and the resulting magnitude or gain (α) and angle (θ) are used to determine the speed and direction of the motor through a percentage pulse width modulation (%PWM) (β) as detailed in Table 2.
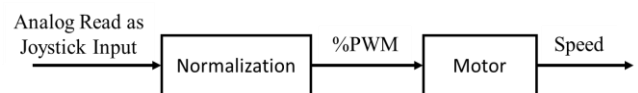
Fig. 14. Block diagram between joystick and motor speed.

A program to control joystick movement can be written based on the processes and equations shown in Fig. 14. These processes and equations describe all necessary conditions and can be used to normalize the analog signal measured from the x-axis and y-axis of the joystick, improving it to a range of -

1 to 1 for determining the scope of movement. This can be done by in (1) and (2).

$$u^X(k) = \frac{input\ analog\ x(k) - 512}{255} \tag{1}$$

$$u^Y(k) = \frac{input\ analog\ y(k) - 512}{255} \tag{2}$$

The coordinates in the X and Y planes (u^X and u^Y) represent the range of movement in those respective planes. To ensure that these coordinates are within the acceptable range, their values are adjusted using in (3) and (4) to be between -1 and 1.

$$\check{u}^X(k) = \begin{cases} 1, & u^X(k) > 1 \\ -1, & u^X(k) < -1 \\ u^X(k), & oterwise \end{cases} \tag{3}$$

where $\check{u}^X$ is the coordinate range in the x-plane that ranges from -1 to 1.

$$\check{u}^Y(k) = \begin{cases} 1, & u^Y(k) > 1 \\ -1, & u^Y(k) < -1 \\ u^Y(k), & oterwise \end{cases} \tag{4}$$

where $\check{u}^Y$ is a coordinate range in the Y-plane that ranges from -1 to 1.

An equation for normalizing the analog joystick system to determine the resultant vector and the angle generated by the joystick is shown in (5), where θ represents the angle produced by the joystick and α represents the resultant vector. The conditions for different angles are expressed in (6).

$$\theta(k) = \begin{cases} 90, & [\check{u}^X(k) = 0\ and\ \check{u}^Y(k) > 0] \\ 270, & [\check{u}^X(k) = 0\ and\ \check{u}^Y(k) < 0] \\ 0, & [\check{u}^X(k) = 0\ and\ \check{u}^Y(k) = 0] \\ \tan^{-1}\left(\frac{\check{u}^Y(k)}{\check{u}^X(k)}\right), & [\check{u}^X(k) > 0\ and\ \check{u}^Y(k) \geq 0] \\ 180 + \left(\tan^{-1}\left(\frac{\check{u}^Y(k)}{\check{u}^X(k)}\right)\right), & [\check{u}^X(k) < 0\ and\ \check{u}^Y(k) \geq 0] \\ 180 + \left(\tan^{-1}\left(\frac{\check{u}^Y(k)}{\check{u}^X(k)}\right)\right), & [\check{u}^X(k) < 0\ and\ \check{u}^Y(k) \leq 0] \\ 360 + \left(\tan^{-1}\left(\frac{\check{u}^Y(k)}{\check{u}^X(k)}\right)\right), & [\check{u}^X(k) > 0\ and\ \check{u}^Y(k) \leq 0] \end{cases} \tag{5}$$

$$\alpha(k) = \begin{cases} \dfrac{\check{u}^Y(k)}{\sin(\theta(k))}, & [\check{u}^X(k) = 0] \\ \dfrac{\check{u}^Y(k)}{\cos(\theta(k))}, & [\check{u}^X(k) \neq 0] \end{cases} \tag{6}$$

The equation for determining the percentage pulse width modulation (%PWM) supply to the motor can be expressed as (7).

$$\beta(k) = \begin{cases} (|\alpha(k)| \times \gamma \times 255), & |\alpha(k)| > 0.1 \\ 0, & |\alpha(k)| \leq 0.1 \end{cases} \tag{7}$$

where β represents the %PWM value, and γ represents the motor power gain, which can be set between 0 and 1 (corresponding to a motor utilization of 0-100%).

2. Mecanum Wheel Control

Mecanum wheel control involves the use of four mecanum wheels and the application of conditions and in (8) to (23) to control their movement in different directions based on the resultant vector of motion. To control the movement of an electric wheelchair equipped with mecanum wheels, four sets of DC motors must be used to determine the direction of rotation for the wheels. The direction of the wheelchair's movement is determined by the combined vectors of these four motors, which apply force to all four wheels when their directions are changed. If the motors are set to the same speed, the resulting force will be equal in all directions. The combination of the vectors of the freely rotating wheels generates a resultant force that determines the direction of movement for the electric wheelchair.

Fig. 15 illustrates the basic structure of the alignment and displacement of four wheels, showing the torque applied to each wheel (T_1, T_2, T_3, T_4). Various movements, such as moving forward (a), moving backward (b), sliding left (c), sliding right (d), turning right (e), and turning left (f), can be achieved through the distribution of forces among the vectors, as shown in Fig. 16.
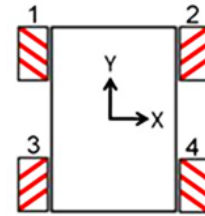
Fig. 15. The alignment of the four wheels.

(a) Forward   (b) Backward   (c) Slide left

(d) Slide right   (e) Turn right   (f) Turn left
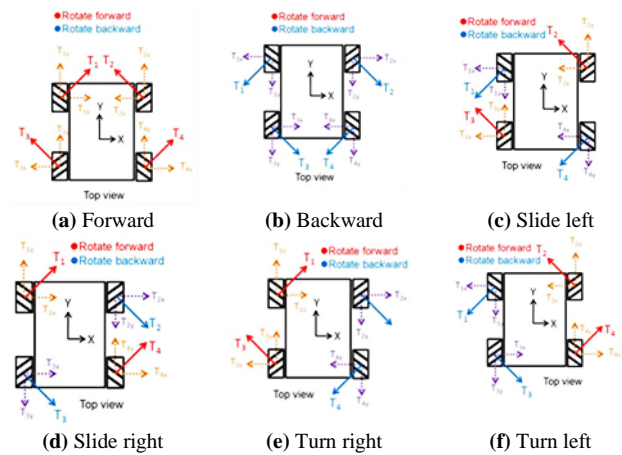
Fig. 16. The direction of movement of the mecanum wheel.

These equations, shown as (8), (9), (10), (11), and (12), can be used to calculate the necessary forces for various movements. Fig. 16 shows the equations for the forces generated in each wheel, which can be used to determine the resultant force of the motors used to propel the electric wheelchair.

$$T_1(k) = \begin{cases} (\%(PWM\ of\ T_1)\angle 45°), & motor\ T_1\ in\ forward \\ (\%(PWM\ of\ T_1)\angle 225°), & motor\ T_1\ in\ reverse \\ (0), & motor\ T_1\ in\ stop \end{cases} \tag{8}$$

$$T_2(k) = \begin{cases} (\%(PWM\ of\ T_2) \angle 135°) , motor\ T_2\ in\ forward \\ (\%(PWM\ of\ T_2) \angle 315°) , motor\ T_2\ in\ reverse \\ (0) , motor\ T_2\ in\ stop \end{cases} \quad (9)$$

$$T_3(k) = \begin{cases} (\%(PWM\ of\ T_3) \angle 135°) , motor\ T_3\ in\ forward \\ (\%(PWM\ of\ T_3) \angle 215°) , motor\ T_3\ in\ reverse \\ (0) , motor\ T_3\ in\ stop \end{cases} \quad (10)$$

$$T_4(k) = \begin{cases} (\%(PWM\ of\ T_4) \angle 45°) , motor\ T_4\ in\ forward \\ (\%(PWM\ of\ T_4) \angle 225°) , motor\ T_4\ in\ reverse \\ (0) , motor\ T_1\ in\ stop \end{cases} \quad (11)$$

$$T_{sum}(k) = \sqrt{T_1(k)^2 + T_2(k)^2 + T_3(k)^2 + T_4(k)^2} \quad (12)$$

Where T_1, T_2, T_3, T_4 and T_{sum} are the sub-forces in each direction and the resultant force in the drive of the mechanum wheel, respectively.

In these equations, T_1, T_2, T_3, T_4 represent the sub-forces in each direction, and T_{sum} represents the resultant force in the drive of the mechanum wheel.

In (13), (14), (15), (16), and (17) represent the resultant forces in the x-axis plane for T_1, T_2, T_3, T_4 and T_{sum}, respectively.

$$T_{1x}(k) = \begin{cases} (\%(PWM\ of\ T_1)) \cos(45) , motor\ T_1\ in\ forward \\ (\%(PWM\ of\ T_1) \cos(225)) , motor\ T_1\ in\ reverse \\ (0) , motor\ T_1\ in\ stop \end{cases} \quad (13)$$

$$T_{2x}(k) = \begin{cases} (\%(PWM\ of\ T_2)) \cos(135) , motor\ T_2\ in\ forward \\ (\%(PWM\ of\ T_2) \cos(315)) , motor\ T_2\ in\ reverse \\ (0) , motor\ T_1\ in\ stop \end{cases} \quad (14)$$

$$T_{3x}(k) = \begin{cases} (\%(PWM\ of\ T_3)) \cos(135) , motor\ T_3\ in\ forward \\ (\%(PWM\ of\ T_3) \cos(315)) , motor\ T_3\ in\ reverse \\ (0) , motor\ T_1\ in\ stop \end{cases} \quad (15)$$

$$T_{4x}(k) = \begin{cases} (\%(PWM\ of\ T_4)) \cos(45) , motor\ T_4\ in\ forward \\ (\%(PWM\ of\ T_4) \cos(225)) , motor\ T_4\ in\ reverse \\ (0) , motor\ T_4\ in\ stop \end{cases} \quad (16)$$

$$T_{sum\ x}(k) = T_{1x}(k) + T_{2x}(k) + T_{3x}(k) + T_{4x}(k) \quad (17)$$

In these equations, T_{1x}, T_{2x}, T_{3x} and T_{4x} represent the x-axis coordinates of T_1, T_2, T_3 and T_4, respectively. $T_{sum\ x}$ represents the sum of the coordinates of the resultant force in the x-axis.

In (18), (19), (20), (21), and (22) represent the resultant forces in the y plane for T_1, T_2, T_3, T_4 and T_{sum}, respectively.

$$T_{1y}(k) = \begin{cases} (\%(PWM\ of\ T_1)) \sin(45) , motor\ T_1\ in\ forward \\ (\%(PWM\ of\ T_1) \sin(225)) , motor\ T_1\ in\ reverse \\ (0) , motor\ T_1\ in\ stop \end{cases} \quad (18)$$

$$T_{2y}(k) = \begin{cases} (\%(PWM\ of\ T_2)) \sin(135) , motor\ T_2\ in\ forward \\ (\%(PWM\ of\ T_2) \sin(315)) , motor\ T_2\ in\ reverse \\ (0) , motor\ T_2\ in\ stop \end{cases} \quad (19)$$

$$T_{3y}(k) = \begin{cases} (\%(PWM\ of\ T_3)) \sin(135) , motor\ T_3\ in\ forward \\ (\%(PWM\ of\ T_3) \sin(315)) , motor\ T_3\ in\ reverse \\ (0) , motor\ T_3\ in\ stop \end{cases} \quad (20)$$

$$T_{4y}(k) = \begin{cases} (\%(PWM\ of\ T_4)) \sin(45) , motor\ T_4\ in\ forward \\ (\%(PWM\ of\ T_4) \sin(225)) , motor\ T_4\ in\ reverse \\ (0) , motor\ T_4\ in\ stop \end{cases} \quad (21)$$

$$T_{sum\ y}(k) = T_{1y}(k) + T_{2y}(k) + T_{3y}(k) + T_{4y}(k) \quad (22)$$

In these equations, T_{1y}, T_{2y}, T_{3y} and T_{4y} represent the y-axis coordinates of the resultant force for T_1, T_2, T_3 and T_4, respectively. $T_{sum\ y}$ represents the sum of the y-axis coordinates of the resultant force.

The angle of movement for the electric wheelchair can be calculated using (23).

$$\theta_{sum}(k) = \tan^{-1} \frac{T_{sum\ y}(k)}{T_{sum\ x}(k)} \quad (23)$$

In this equation, θ_{sum} represents the direction of the resultant force of electric wheelchair movement. To determine the direction of movement for the electric wheelchair, the direction of rotation for the motors can be determined using Table 2, which defines the motion conditions for the mechanum wheels to move in the desired direction. This table provides information on the necessary motor conditions for T_1, T_2, T_3 and T_4 to move the electric wheelchair in the desired direction.

TABLE II. SHOWS THE DIRECTION OF MOVEMENT AND THE ACTIVATION OF THE WHEEL ROTATION.

	T_1	T_2	T_3	T_4
Forward	forward	forward	forward	forward
Backward	reverse	reverse	reverse	reverse
Slide left	reverse	forward	forward	reverse
Slide right	forward	reverse	reverse	forward
Turn right	forward	reverse	forward	reverse
Turn left	reverse	forward	reverse	forward

To summarize this section, Fig. 11 shows the relationship between joystick control and mechanum wheel movement. To use joystick control, the magnitude or gain (α) and angle (θ) of the movement must be determined, and a percentage pulse width modulation (%PWM) (β) must be applied to set the speed of the motor and position of the movement to the control wheelchair in Table 2.

III. AVERAGE FILTER

A moving average, or average filter, is a statistical method used to analyze data by creating a series of averages from different subsets of the full dataset. This method allows for the identification of trends and patterns in the data, as well as the smoothing of fluctuations or noise in the data. It is often used in time series analysis to help identify trends and make predictions about data points. This is typically represented by (24).

$$y_{avg}(k) = \frac{1}{N} \sum_{k-N}^{k} x_{input} \quad (24)$$

where y_{avg} is the output of the average, x_{input} is the data input, N is the number of data points used to calculate the average, and k is the step time.

In this equation, the moving average filter calculates the average of a certain number of data points at each step time. In this research, input data were collected in 10 data, with a sampling time of 50 ms. The values of α and θ were estimated by normalizing the data to inputs in the average filter.

IV. RESULTS AND DISCUSSION

This chapter covers the system testing of different parts of an analog joystick, including the direction of movement of the mecanum wheel. These tests follow ISO 2570-2555 standards and are intended to confirm that the system is functioning correctly and meets all required specifications.

The following sections describe these components in more detail.

A. Joystick Testing

1. Testing I

Joystick testing was conducted on each axis (analog x and analog y) to normalize the block and determine the magnitude or gain (α) and angle (θ) of the joystick movement as shown in Fig. 3 and Fig. 14. The results of each angle can be seen in Table 3, and Fig. 17 shows the x and y coordinates to represent the resulting vector on a unit circle. This testing was done to ensure that the joystick is functioning properly and accurately controlling the movement of the electric wheelchair.
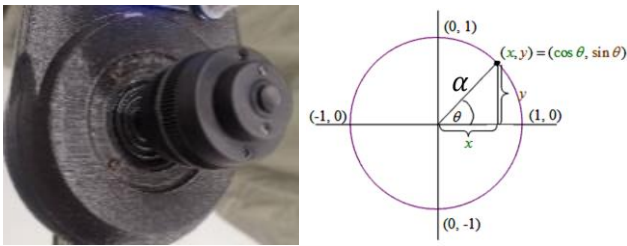
Fig. 17. Joystick and unit circle.

TABLE III. SHOWS THE ANALOG JOYSTICK TESTING VALUE.

No	Gain (α)	Angle (°)	Data of Joystick Reading (°)	Error (°)
1	1	0	0.00	0.00
2	1	30	30.12	-0.12
3	1	60	60.35	-0.35
4	1	90	90.00	0.00
5	1	120	120.15	-0.15
6	1	150	150.05	-0.05
7	1	180	180.00	0.00
8	1	210	210.29	-0.29
9	1	240	240.18	-0.18
10	1	270	270.00	0.00
11	1	300	300.66	-0.66
12	1	330	330.22	-0.22
Average				-0.17

According to Table 3, the joystick was able to accurately display the angle and detect the tilt position, with an average error of -0.17 degrees. It is worth noting that this small discrepancy may be influenced by the wheelchair user's ability to precisely control the angle of the joystick while in motion.

2. Testing II

In testing 2, a joystick controller was used to test the system. The positions of α and θ were set to approximately 0.94 units and 176.65 degrees, respectively. The joystick controller was held in place for 5 seconds, and the estimated values from (24) were compared with those obtained when the average filter was not used. The results of this comparison are shown in Fig. 18 and Fig. 19.

The results of the experiment, shown in Fig. 18 and Fig. 19, indicate that the use of an average filter resulted in a significant reduction in the fluctuation in the signal magnitude or gain (α) and angle (θ). Without the use of the average filter, the magnitude (α) had a fluctuation of about 0.

01 units and the angle (θ) had a fluctuation of about 0.25 degrees.
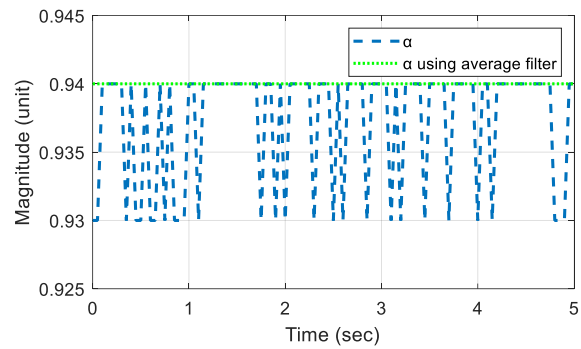
Fig. 18. The results of α in relation to joystick was held in place for 5 sec.
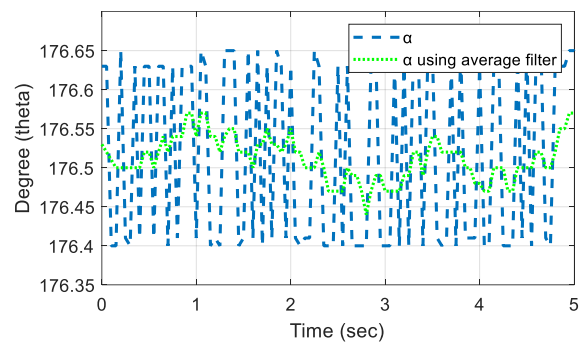
Fig. 19. The results of θ in relation to joystick was held in place for 5 sec.

However, when the average filter was applied, the magnitude (α) remained relatively stable with only a small amount of fluctuation, and the angle (θ) had a fluctuation of about 0.1 degrees. These findings suggest that the average filter can improve the stability and accuracy of the system by reducing fluctuations in the data.

3. Testing III

In testing 3, the joystick controller was tested by moving it to different coordinates within its range of movement for a duration of 15 seconds. The test was then terminated by releasing the joystick. The results of this experiment are depicted in Fig. 20, Fig. 21, and Fig. 22.
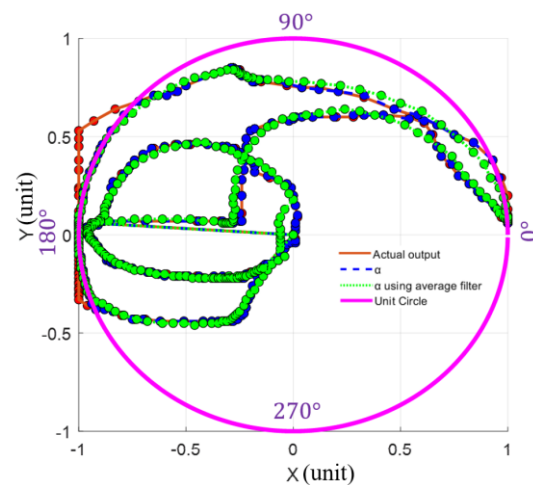
Fig. 20. The results of joystick movement.
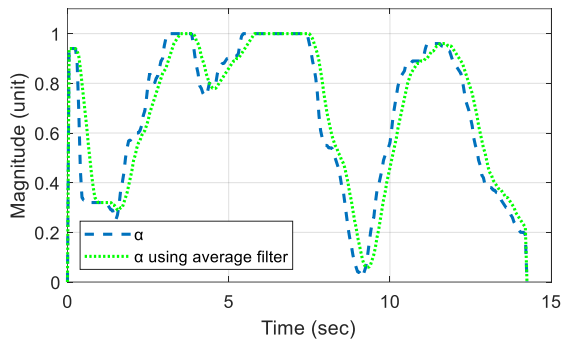
Fig. 21. The results of α in relation to movement.
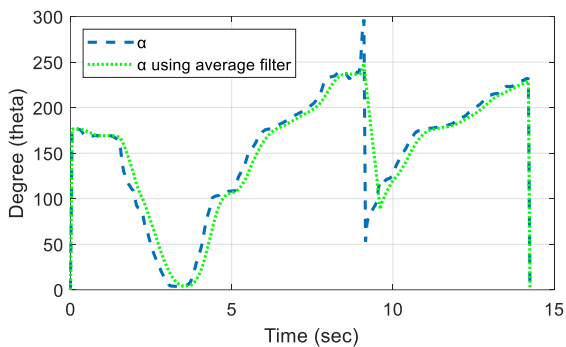
Fig. 22. The results of θ in relation to movement.

According to the results of the system tests shown in Fig. 20, the data is plotted on the XY coordinate system. The unit circle boundary is represented by a purple line, the actual output value is shown by a red line, the value of α is represented by a blue line, and the value of α using the average filter is shown by a green line. The actual output shows movement both within and outside the 1-unit circle coordinates. The approximated values of α obtained from normalization are only within the 1-unit circle coordinates, including the value of α using the average filter. When comparing Fig. 21 and Fig. 22, it can be seen that the value of α using the average filter has some derating, but the approximation of α using the average filter has a smoother signal. When applied to the control of electric wheelchairs, this will result in a more stable speed and angle control.

B. Mecanum Wheel for Electric Wheelchair Testing

The mobility of the electric wheelchair was tested and found to be able to move forward, backward, turn left, and turn right, as well as move the slider to the left and right sides of the chair as shown in Fig. 23, Fig. 24, Fig. 25, Fig. 26, Fig. 27, and Fig. 28. The speed at which the motors and electric wheelchair move is determined by the size of the analog joystick rocker, which is programmed into the system using (7) and the system's programming as shown in Fig. 11. Although the system is designed to work as an open-loop control system, it is still able to effectively utilize the capabilities of the mecanum wheels on both smooth and uneven surfaces.

Fig. 23. Forward testing of the electric wheelchair.
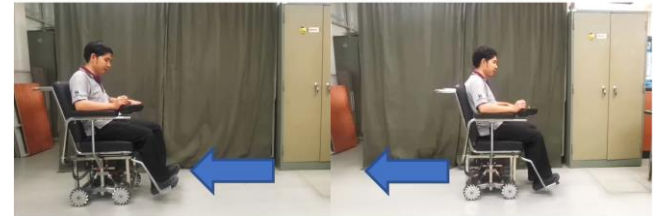
Fig. 24. Backward testing of the electric wheelchair.

Fig. 25. Turn left testing of the electric wheelchair.

Fig. 26. Turn right testing of the electric wheelchair.
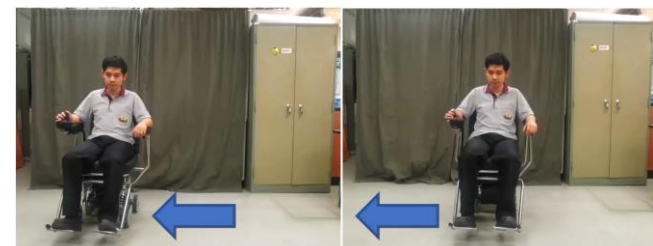
Fig. 27. Slide right testing of the electric wheelchair.
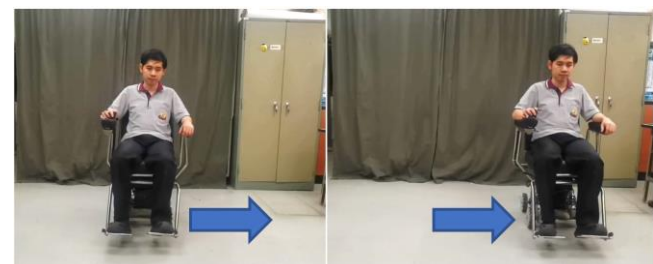
Fig. 28. Slide left testing of the electric wheelchair.

C. Pats ISO 2570-2555 standards Testing

For the test results in terms of conformity to the requirements of ISO standards. 2027-2012 has shown the test results as shown in Table 4. In addition, for the test in terms of maximum load, battery charging system, strength test, impact test, and durability test, as well as the test results on incline movement of 5 m at an incline of 7 degrees by in a virtual environment in the laboratory, it was found that the electric wheelchairs that had been designed and built had passed the test in all such conditions.

TABLE IV. SYSTEM TESTING FOLLOWS ISO 2570 – 2555

Test Number	Detail	Results
1	The maximum user mass does not exceed 100 kg.	Success
2	Cart size (largest dimension)	Success
3	Battery charging system	Success
4	Stable structure	Success
5	Strength, impact and durability testing	Success
6	Test run on inclined ground, distance 5 m, tilt angle 7°	Success

Overall, our electric wheelchair design is simple, reliable, and cost-effective, with a price tag of no more than 40, 000 Thai Baht. The joystick, which is powered by an Arduino microcontroller, effectively controls the movement of the wheels and performs as expected. This design offers a low-cost solution for those in need of an electric wheelchair.

V. CONCLUSION

In conclusion, the electric wheelchair designed in this research was found to meet the research objectives in terms of movement and maintenance. It was able to move like a conventional electric wheelchair and was able to support weights of up to 100 kg. The tools needed for maintenance were found to be readily available within the country, and certain parts could be disassembled and replaced by the user. The four wheels were evenly distributed, allowing the wheelchair to effectively navigate smooth surfaces, although rough surfaces may cause damage to the rubber wheels and should be avoided. The joystick had a maximum error rate of -0. 17 degrees, and the use of the average filter improved the processing of the joystick. For future work, it is recommended to consider using DC motors with feedback control to maintain constant speed when battery levels change and to design a closed loop control system to ensure constant speed control, even when battery power fluctuates, and to enable a smooth start using speed profile.

REFERENCES

[1] M. Z. Mistarihi, "A data set on anthropometric measurements and degree of discomfort of physically disabled workers for ergonomic requirements in work space design," *Data in brief*, vol. 30, 2020.

[2] C. J. Tu, L. Liu, W. Wang, H. P. Du, Y. M. Wang, Y. B. Xu, and P. Li, "Effectiveness and safety of wheelchair skills training program in improving the wheelchair skills capacity: a systematic review," *Clinical rehabilitation*, vol. 31, no. 12, pp. 1573-1582, 2017.

[3] R. Gartz, M. Goldberg, A. Miles, R. Cooper, J. Pearlman, M. Schmeler, and J. Hale, "Development of a contextually appropriate, reliable and valid basic Wheelchair Service Provision Test," *Disability and Rehabilitation: Assistive Technology*, vol. 12, no. 4, pp. 333-340, 2017.

[4] G. V. Henderson, M. L. Boninger, B. E. Dicianno, and L. A. Worobey, "Type and frequency of wheelchair repairs and resulting adverse consequences among veteran wheelchair users," *Disability and Rehabilitation: Assistive Technology*, vol. 17, no. 3, pp. 331-337, 2022.

[5] T. E. Nightingale, P. C. Rouse, D. Thompson, and J. L. Bilzon, "Measurement of physical activity and energy expenditure in wheelchair users: methods, considerations and future directions," *Sports medicine-open*, vol. 3, no. 1, pp. 1-16, 2017.

[6] E. McSweeney and R. J. Gowran, "Wheelchair service provision education and training in low and lower middle income countries: a scoping review," *Disability and Rehabilitation: Assistive Technology*, vol. 14, no. 1, pp. 33-45, 2019.

[7] M. Toro, R. Gartz, M. Goldberg, P. Rushton, N. Seymour, K. Fung, and J. Pearlman, "Wheelchair service provision education in academia," *African Journal of Disability*, vol. 6, no. 1, pp. 1-8, 2017.

[8] R. Velho, "Transport accessibility for wheelchair users: A qualitative analysis of inclusion and health," *International Journal of Transportation Science and Technology*, vol. 8, no. 2, pp. 103-115, 2019.

[9] P. Geoerg, J. Schumann, S. Holl, and A. Hofmann, "The influence of wheelchair users on movement in a bottleneck and a corridor," *Journal of advanced transportation*, vol. 2019, 2019.

[10] E. Williams, E. Hurwitz, I. Obaga, B. Onguti, A. Rivera, T. R. L. Sy, and E. Bazant, "Perspectives of basic wheelchair users on improving their access to wheelchair services in Kenya and Philippines: a qualitative study," *BMC international health and human rights*, vol. 17, no. 1, pp. 1-12, 2017.

[11] A. Ma'arif and A. Çakan, "Simulation and Arduino hardware implementation of dc motor control using sliding mode controller," *Journal of Robotics and Control (JRC)*, vol. 2, no. 6, pp. 582-587, 2021.

[12] A. Ma'arif and N. R. Setiawan, "Control of DC motor using integral state feedback and comparison with PID: simulation and Arduino implementation," *Journal of Robotics and Control (JRC)*, vol. 2, no. 5, pp. 456-461, 2021.

[13] M. Saad, A. H. Amhedb, and M. Al Sharqawi, "Real time DC motor position control using PID controller in LabVIEW," *Journal of Robotics and Control (JRC)*, vol. 2, no. 5, pp. 342-348, 2021.

[14] A. A. Mohammed, A. Abdullahi, and A. Ibrahim, "Development of a Prototype Autonomous Electric Vehicle," *Journal of Robotics and Control (JRC)*, vol. 2, no. 6, pp. 559-564, 2021.

[15] J. Susilo, A. Febriani, U. Rahmalisa, and Y. Irawan, "Car parking distance controller using ultrasonic sensors based on Arduino uno," *Journal of Robotics and Control (JRC)*, vol. 2, no. 5, pp. 353-356, 2021.

[16] A. R. Al Tahtawi, M. Agni, and T. D. Hendrawati, "Small-scale Robot Arm Design with Pick and Place Mission Based on Inverse Kinematics," *Journal of Robotics and Control (JRC)*, vol. 2, no. 6, pp. 469-475, 2021.

[17] M. R. Islam, M. R. T. Hossain, and S. C. Banik, "Synchronizing of stabilizing platform mounted on a two-wheeled robot," *Journal of Robotics and Control (JRC)*, vol. 2, no. 6, pp. 552-558, 2021.

[18] C. Iwendi, M. A. Alqarni, J. H. Anajemba, A. S. Alfakeeh, Z. Zhang, and A. K. Bashir, "Robust navigational control of a two-wheeled self-balancing robot in a sensed environment," *IEEE Access*, vol. 7, pp. 82337-82348, 2019.

[19] F. A. Raheem, B. F. Midhat, and H. S. Mohammed, "PID and fuzzy logic controller design for balancing robot stabilization," *Iraqi Journal of Computers, Communications, Control and Systems Engineering*, vol. 18, no. 1, pp. 1-10, 2018.

[20] F. Jiménez, I. Ruge, and A. Jiménez, "Modeling and Control of a Two Wheeled Self-Balancing Robot: a didactic platform for control engineering education," *LACCEI Inc.*, 2020.

[21] I. Gandarilla, V. Santibañez, and J. Sandoval, "Control of a self-balancing robot with two degrees of freedom via IDA-PBC," *ISA transactions*, vol. 88, pp. 102-112, 2019.

[22] Y. Su, T. Wang, K. Zhang, C. Yao, and Z. Wang, "Adaptive nonlinear control algorithm for a self-balancing robot," *IEEE Access*, vol. 8, pp. 3751-3760, 2019.

[23] S. D. Perkasa, P. Megantoro, and H. A. Winarno, "Implementation of a camera sensor pixy 2 CMUcam5 to a two wheeled robot to follow colored object," *Journal of Robotics and Control (JRC)*, vol. 2, no. 6, pp. 469-501, 2021.

[24] A. Latif, A. Z. Arfianto, J. E. Poetro, T. N. Phong, and E. T. Helmy, "Temperature Monitoring System for Baby Incubator Based on Visual Basic," *Journal of Robotics and Control (JRC)*, vol. 2, no. 1, pp. 47-50, 2021.

[25] M. Hinderer, P. Friedrich, and B Wolf, "An autonomous stair-climbing wheelchair," *Robotics and autonomous systems*, vol. 94, pp. 219-225, 2017.

[26] P. Chotikunnan and B. Panomruttanarug, "The application of fuzzy logic control to balance a wheelchair," *Journal of control engineering and applied informatics*, vol. 18, no. 3, pp. 41-51, 2016.

[27] C. Ma, W. Li, R. Gravina, and G. Fortino, "Posture detection based on smart cushion for wheelchair users," *Sensors*, vol. 17, no. 4, pp. 719, 2017.

[28] A. Alshaer, H. Regenbrecht, and D. O'Hare, "Immersion factors affecting perception and behaviour in a virtual reality power wheelchair simulator," *Applied ergonomics*, vol. 58, pp. 1-12, 2017.

[29] N. W. John, S. R. Pop, T. W. Day, P. D. Ritsos, and C. J. Headleand, "The implementation and validation of a virtual environment for training powered wheelchair manoeuvres," *IEEE transactions on visualization and computer graphics*, vol. 24, no. 5, pp. 1867-1878, 2017.

[30] S. Arlati, V. Colombo, G. Ferrigno, R. Sacchetti, and M. Sacco, "Virtual reality-based wheelchair simulators: A scoping review," *Assistive Technology*, vol. 32, no. 6, pp. 294-305, 2020.

[31] Y. Morère, G. Bourhis, K. Cosnuau, G. Guilmois, E. Rumilly, and E. Blangy, "ViEW: a wheelchair simulator for driving analysis," *Assistive technology*, vol. 32, no. 3, pp. 125-135, 2018.

[32] L. Yang, N. Guo, R. Sakamoto, N. Kato, and K. I. Yano, "Electric Wheelchair Hybrid Operating System Coordinated with Working Range of a Robotic Arm," *Journal of Robotics and Control (JRC)*, vol. 3, no. 5, pp. 679-689, 2022.

[33] A. Hartman and V. K. Nandikolla, "Human-machine interface for a smart wheelchair," *Journal of Robotics*, vol. 2019. 2019.

[34] W. Szaj, P. Fudali, W. Wojnarowska, and S. Miechowicz, "Mechatronic Anti-Collision System for Electric Wheelchairs Based on 2D LiDAR Laser Scan," *Sensors*, vol. 21, no. 24, 2021.

[35] O. Piña-Ramirez, R. Valdes-Cristerna, and O. Yanez-Suarez, "Scenario screen: A dynamic and context dependent P300 stimulator screen aimed at wheelchair navigation control," *Computational and mathematical methods in medicine*, vol. 2018. 2018.

[36] A. Mobasheri, J. Deister, and H. Dieterich, "Wheelmap: the wheelchair accessibility crowdsourcing platform," *Open Geospatial Data, Software and Standards*, vol. 2, no. 1, pp. 1-7, 2017.

[37] M. J. Haddad and D. A. Sanders, "Selecting a best compromise direction for a powered wheelchair using PROMETHEE," *IEEE Transactions on Neural Systems and Rehabilitation Engineering*, vol. 27, no. 2, pp. 228-235, 2019.

[38] R. M. A. Van der Slikke, B. S. Mason, M. A. M. Berger, and V. L. Goosey-Tolfrey, "Speed profiles in wheelchair court sports; comparison of two methods for measuring wheelchair mobility performance," *Journal of Biomechanics*, vol. 65, pp. 221-225, 2017.

[39] Y. Rabhi, M. Mrabet, and F. Fnaiech, "A facial expression controlled wheelchair for people with disabilities," *Computer methods and programs in biomedicine*, vol. 165, pp. 89-105, 2018.

[40] Y. Rabhi, M. Mrabet, and F. Fnaiech, "Intelligent control wheelchair using a new visual joystick," *Journal of Healthcare Engineering*, vol. 2018, 2018.

[41] M. Dahmani, M. E. Chowdhury, A. Khandakar, T. Rahman, K. Al-Jayyousi, A. Hefny, and S. Kiranyaz, "An intelligent and low-cost eye-tracking system for motorized wheelchair control," *Sensors*, vol. 20, no. 14, 2020.

[42] H. H. Tesfamikael, A. Fray, I. Mengsteab, A. Semere, and Z. Amanuel, "Simulation of Eye Tracking Control based Electric Wheelchair Construction by Image Segmentation Algorithm," *Journal of Innovative Image Processing (JIIP)*, vol. 3, no. 1, pp. 21-35, 2021.

[43] Q. Huang, S. He, Q. Wang, Z. Gu, N. Peng, K. Li, and Y. Li, "An EOG-based human–machine interface for wheelchair control," *IEEE transactions on biomedical engineering*, vol. 65, no. 9, pp. 2023-2032, 2017.

[44] J. J. Gu, M. Meng, A. Cook, and P. X. Liu, Design, "Sensing and control of a robotic prosthetic eye for natural eye movement," *Applied Bionics and Biomechanics*, vol. 3, no. 1, pp. 29-41, 2006.

[45] S. Mishra, J. J. Norton, Y. Lee, D. S. Lee, N. Agee, Y. Chen, and W. H. Yeo, "Soft, conformal bioelectronics for a wireless human-wheelchair interface," *Biosensors and Bioelectronics*, vol. 91, pp. 796-803, 2017.

[46] R. H. Abiyev, N. Akkaya, E. Aytac, I. Günsel, and A. Çağman, "Brain-computer interface for control of wheelchair using fuzzy neural networks," *BioMed research international*, vol. 2016, 2016.

[47] Z. T. Al- Qaysi, B. B. Zaidan, A. A. Zaidan, and M. S. Suzani, "A review of disability EEG based wheelchair control system: Coherent taxonomy, open challenges and recommendations," *Computer methods and programs in biomedicine*, vol. 164, pp. 221-237, 2018.

[48] M. A. Hadj-Abdelkader, G. Bourhis, and B. Cherki, "Haptic feedback control of a smart wheelchair," *Applied Bionics and Biomechanics*, vol. 9, no. 2, pp. 181-192, 2012.

[49] D. Kumar, R. Malhotra, and S. R. Sharma, "Design and construction of a smart wheelchair," *Procedia Computer Science*, vol. 172, pp. 302-307, 2020.

[50] A. Sharmila, A. Saini, S. Choudhary, T. Yuvaraja, and S. G. Rahul, "Solar Powered Multi-Controlled Smart Wheelchair for Disabled: Development and Features," *Journal of Computational and Theoretical Nanoscience*, vol. 16, no. 11, pp. 4889-4900, 2019.

[51] K. Sukerkar, D. Suratwala, A. Saravade, J. Patil, and R. D'britto, "Smart wheelchair: a literature review," *International Journal of Informatics and Communication Technology (IJ-ICT)*, vol. 5, no. 5. 4, pp. 5-6, 2018.

[52] K. Ajithraj, P. S. Sandeep, E. K. Vipin, K. Harishankar, and M. P. Jijeesh, "Smart Wheelchair Controlled by Brain Waves," *Sreepathy Journal of Electronics and Communication Engineering*, vol. 1, no. 2, 2015.

[53] K. Rahimunnisa, M. Atchaiya, B. Arunachalam, and V. Divyaa, "AI-based smart and intelligent wheelchair," *Journal of applied research and technology*, vol. 18, no. 6, pp. 362-367, 2020.

[54] I. Zeidis and K. Zimmermann, "Dynamics of a four-wheeled mobile robot with Mecanum wheels," *ZAMM-Journal of Applied Mathematics and Mechanics/Zeitschrift für Angewandte Mathematik und Mechanik*, vol. 99, no. 12, 2019.

[55] L. Sang, M. Yamamura, F. Dong, Z. Gan, J. Fu, H. Wang, and Y. Tian, "Analysis, design and experimental research of a novel wheelchair-stretcher assistive robot," *Applied Sciences*, vol. 10, no. 1, 2019.

[56] C. E. O. Lima, "Dynamic Obstacle Avoidance for 4 Wheeled Omni Wheelchair using a New Type of Mecanum Wheel," *International*

Journal of Innovative Science and Research Technology, vol. 4, no. 7, pp. 600-606, 2019.

[57] Y. Li, S. Dai, Y. Zheng, F. Tian, and X. Yan, "Modeling and kinematics simulation of a Mecanum wheel platform in RecurDyn," *Journal of Robotics*, vol. 2018, 2018.

[58] Z. Hendzel and Ł. Rykała, "Modelling of dynamics of a wheeled mobile robot with mecanum wheels with the use of Lagrange equations of the second kind," *International Journal of Applied Mechanics and Engineering*, vol. 22, no. 1, 2017.

[59] Y. Li, S. Dai, L. Zhao, X. Yan, and Y. Shi, "Topological design methods for mecanum wheel configurations of an omnidirectional mobile robot," *Symmetry*, vol. 11, no. 10, 2019.

[60] Y. Li, S. Ge, S. Dai, L. Zhao, X. Yan, Y. Zheng, and Y. Shi, "Kinematic modeling of a combined system of multiple mecanum-wheeled robots with velocity compensation," *Sensors*, vol. 20, no. 1, 2019.

[61] R. O. Isah, O. M. Olaniyi, J. G. Kolo, and D. Z. Babatunde, "A smart omnidirectional controlled wheelchair," *Journal of Engineering Science*, vol. 27, no. 4, pp. 88-102, 2020.

[62] Y. Li, S. Dai, Y. Shi, L. Zhao, and M. Ding, "Navigation simulation of a Mecanum wheel mobile robot based on an improved A* algorithm in Unity3D," *Sensors*, vol. 19, no. 13, 2019.

[63] Z. Yuan, Z. Tian, Y. Yin, S. Wang, J. Liu, and L. Wu, "Trajectory tracking control of a four mecanum wheeled mobile platform: an extended state observer-based sliding mode approach," *IET Control Theory & Applications*, vol. 14, no. 3, pp. 415-426, 2020.

[64] P. S. Yadav, V. Agrawal, J. C. Mohanta, and M. F. Ahmed, "A robust sliding mode control of mecanum wheel-chair for trajectory tracking," *Materials Today: Proceedings*, vol. 56, pp. 623-630, 2022.

[65] H. Yang, S. Wang, Z. Zuo, and P. Li, "Trajectory tracking for a wheeled mobile robot with an omnidirectional wheel on uneven ground," *IET Control Theory & Applications*, vol. 14, no. 7, pp. 921-929, 2020.

[66] S. Duda, O. Dudek, G. Gembalczyk, and T. Machoczek, "Determination of the kinematic excitation originating from the irregular envelope of an omnidirectional wheel," *Sensors*, vol. 21, no. 20, 2021.

[67] J. Palacín, D. Martínez, E. Rubies, and E. Clotet, "Suboptimal omnidirectional wheel design and implementation," *Sensors*, vol. 21, no. 3, 2021.

[68] E. Rubies and J. Palacín, "Design and FDM/FFF Implementation of a Compact Omnidirectional Wheel for a Mobile Robot and Assessment of ABS and PLA Printing Materials," *Robotics*, vol. 9, no. 2, 2020.

[69] R. T. Yunardi, D. Arifianto, F. Bachtiar, and J. I. Prananingrum, "Holonomic implementation of three wheels omnidirectional mobile robot using dc motors," *Journal of Robotics and Control (JRC)*, vol. 2, no. 2, pp. 65-71, 2021.

[70] W. Batayneh and Y. AbuRmaileh, "Decentralized motion control for omnidirectional wheelchair tracking error elimination using PD-fuzzy-P and GA-PID controllers," *Sensors*, vol. 20, no. 12, 2020.

[71] D. U. Rijalusalam and I. Iswanto, "Implementation kinematics modeling and odometry of four omni wheel mobile robot on the trajectory planning and motion control based microcontroller," *Journal of Robotics and Control (JRC)*, vol. 2, no. 5, pp. 448-455, 2021.

[72] C. Kim, J. Suh, and J. H. Han, "Development of a hybrid path planning algorithm and a bio-inspired control for an omni-wheel mobile robot," *Sensors*, vol. 20, no. 15, 2020.

[73] M. Hijikata, R. Miyagusuku, and K. Ozaki, "Wheel Arrangement of Four Omni Wheel Mobile Robot for Compactness," *Applied Sciences*, vol. 12, no. 12, 2022.

[74] C. Cai, J. Lu, and Z. Li, "Kinematic Analysis and Control Algorithm for the Ballbot," *IEEE Access*, vol. 7, pp. 38314–38321, 2019.

[75] P. Van Lam and Y. Fujimoto, "A Robotic Cane for Balance Maintenance Assistance," *IEEE Trans. Ind. Informatics*, vol. 15, no. 7, pp. 3998–4009, Jul. 2019.

[76] W. Li and R. Xiong, "Dynamical Obstacle Avoidance of TaskConstrained Mobile Manipulation Using Model Predictive Control," *IEEE Access*, vol. 7, pp. 88301–88311, 2019.

[77] T. Terakawa, M. Komori, K. Matsuda, and S. Mikami, "A Novel Omnidirectional Mobile Robot with Wheels Connected by Passive Sliding Joints," *IEEE/ASME Trans. Mechatronics*, vol. 23, no. 4, pp. 1716–1727, Aug. 2018.

[78] P. Shen, X. Zhang, and Y. Fang, "Complete and Time-Optimal PathConstrained Trajectory Planning with Torque and Velocity Constraints: Theory and Applications," *IEEE/ASME Trans. Mechatronics*, vol. 23, no. 2, pp. 735–746, Apr. 2018.

[79] M. A. Al Mamun, M. T. Nasir, and A. Khayyat, "Embedded System for Motion Control of an Omnidirectional Mobile Robot," *IEEE Access*, vol. 6, no. 8, pp. 86722–6739, 2018.

[80] M. Ferro, A. Paolillo, A. Cherubini, and M. Vendittelli, "VisionBased Navigation of Omnidirectional Mobile Robots," *IEEE Robot. Autom. Lett.*, vol. 4, no. 3, pp. 2691–2698, Jul. 2019.

[81] B. A. Gebre and K. V. Pochiraju, "Machine Learning Aided Design and Analysis of a Novel Magnetically Coupled Ball Drive," *IEEE/ASME Trans. Mechatronics*, vol. 24, no. 5, pp. 1942–1953, Oct. 2019.